

# **Emission Impact Potential – A Method for Relating Upwind Emissions to Ambient Pollutant Concentrations**

Sean M. Raffuse, Dana C. Sullivan, and Lyle R. Chinkin  
Sonoma Technology, Inc.  
1360 Redwood Way, Suite C, Petaluma, CA 94954  
sraffuse@sonomatech.com

## **ABSTRACT**

In support of the Central States Regional Air Planning Association's (CENRAP) need to develop a regional haze plan, Sonoma Technology, Inc. (STI) analyzed meteorological data and emission inventories to evaluate potential contributors (i.e., emissions source types and geographic source regions) to episodes of poor and good visibility at Hercules Glades Wilderness in Missouri. A geographic information systems- (GIS) based tool was developed to facilitate and automate elements of these analyses. County-level emissions were weighted by the frequency and residence time of modeled backward trajectories passing over each county to estimate the potential for emissions from each county to impact the site. This is called the emission impact potential (EIP). This simple analysis technique is useful for characterizing general patterns and developing a preliminary conceptual model of factors affecting visibility conditions before full-scale photochemical modeling efforts are carried out. The preliminary study concentrated on emissions of NO<sub>x</sub> and SO<sub>2</sub>. For both pollutants, the relative contribution of different source types was not significantly different between good and poor visibility days; however, source regions (i.e., counties contributing the most to EIP) varied substantially.

## **INTRODUCTION**

The Central States Regional Air Planning Association (CENRAP) is responding to the U.S. Environmental Protection Agency's (EPA's) mandate to protect visibility in Class I areas by researching visibility-related issues and developing a regional haze plan for the CENRAP region, which includes Texas, Oklahoma, Louisiana, Arkansas, Kansas, Missouri, Nebraska, Iowa, and Minnesota. In order to produce an effective regional haze plan, the CENRAP must develop a conceptual model of the phenomena that lead to episodes of low and high visibility in the states in the CENRAP region. CENRAP needs information that can be used for planning photochemical modeling assessments, including selection of episodes, geographic areas, and effective control strategies to be modeled.

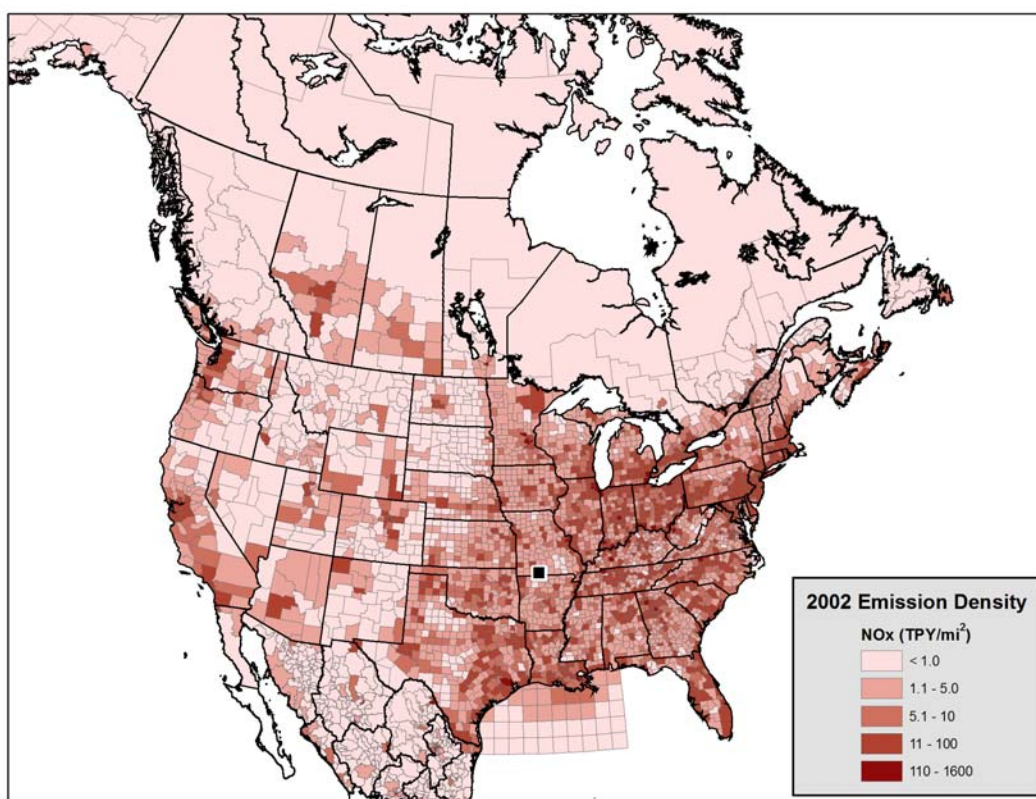
Backward-trajectory analyses have been applied in various air quality studies to examine potential sources of measured pollutants at a receptor site<sup>1-5</sup>. Source regions identified by backward-trajectory techniques can be compared to emissions data maps to verify that the pollutants (or their precursors) measured at the receptor site are emitted in those regions. To fully explore the relationship among emissions, atmospheric dynamics, and measured concentrations, photochemical modeling can be employed. However, modeling is expensive and time consuming and is thus typically applied to selected case studies. As a preliminary screening analysis, we employed a simple method to mathematically combine emission inventory data with a backward-trajectory ensemble technique. This technique, called emission impact potential (EIP), shows the potential of individual source areas to contribute to downwind pollution based on emission inventories and air mass trajectories alone.

## METHODS

### Emission Inventory

Emission inventory data for 2002 were acquired for the United States, Canada, northern Mexico, and the Gulf of Mexico from the regional planning organizations and other sources. Information about the criteria pollutants ( $\text{NO}_x$ ,  $\text{SO}_2$ ,  $\text{PM}_{10}$ ,  $\text{PM}_{2.5}$ ,  $\text{NH}_3$ ,  $\text{CO}$ , and  $\text{VOC}$ ) was collected into a single North American emission inventory in a SQL Server database. The inventory was resolved on a county level for the United States, on a regional municipality level for Canada, on a municipio level for Mexico, and on a one-degree grid for the Gulf of Mexico. For Canada, emissions information was only available at the province level. These were allocated to the municipality level using population density. Figure 1 is a map of  $\text{NO}_x$  emission density from the developed inventory.

**Figure 1.** 2002 North American emission inventory  $\text{NO}_x$  emission density.



### Spatial Probability Density

The National Oceanic and Atmospheric Administration (NOAA) HYbrid Single-Particle Lagrangian Integrated Trajectory (HYSPLIT) model<sup>6</sup> was used to determine transport patterns to the receptor site. An ensemble of backward trajectory model runs was performed to represent the various possible wind patterns on each day of interest. For visibility protected (Class I) areas such as Hercules Glades Wilderness the days with the 20%-worst and the 20%-best visibility are of most interest. Data from the Interagency Monitoring of Protected Visual Environments (IMPROVE) network for every third day from March 2001 through 2003 were used to determine the dates of best and worst visibility. The

parameters used to run the trajectories are shown in Table 1. The trajectories were limited to 72-hr endpoints to minimize model uncertainties.

**Table 1.** Parameters used to run the NOAA HYSPLIT model.

Parameter	Value
Starting heights	50, 300, 700 m
Run time	72 hours
Minimum valid data points	75%
Starting hours	0, 4, 8, 12, 16, 20
Top of model	10,000 m
Model data	EDAS
Vertical motion	Isobaric

The hourly points from all trajectories over all days of interest are combined using the Spatial Probability Density ( $D_0$ ), which is a kernel density of all hourly trajectory points, normalized to a maximum value of one:

$$\text{Equation (1)} \quad D_0 = \frac{D_c}{\hat{D}}$$

where

$D_c$  = Density at grid cell  $c$

$\hat{D}$  = Maximum density over all grid cells (density at receptor site)

$$\text{Equation (2)} \quad D_c = \sum_{i=1}^n \kappa_R(r_n)$$

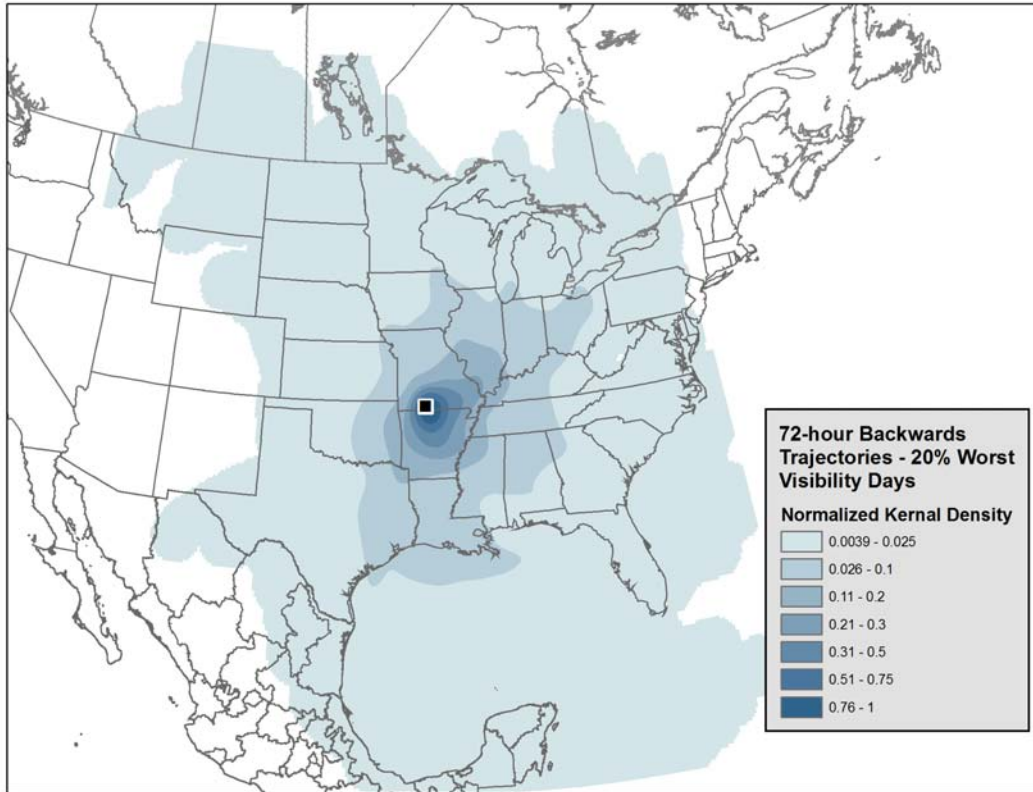
where  $r_n$  = distance between grid cell center and hourly trajectory point  $n$

$$\kappa_R(r) = \text{kernal density function} = \begin{cases} \frac{3}{\pi R^2} \left[ 1 - \left( \frac{r}{R} \right)^2 \right] & \text{for } r < R \\ 0 & \text{for } r \geq R \end{cases}$$

$R$  = search radius

The search radius  $R$  was determined dynamically by dividing the geographic extent of all hourly trajectory points by 30<sup>7,8</sup>. Figure 2 shows the spatial probability density map for poor visibility days at Hercules Glades Wilderness. A value of one indicates that all trajectories pass near the grid cell, while a value closer to zero denotes an area over which very few trajectories passed.

**Figure 2.** Spatial Probability Density for Hercules Glades Wilderness on the 20% worst visibility days.



### Emission Impact Potential (EIP)

The Spatial Probability Density is used to weight the emissions from individual counties and estimate the potential for specific upwind areas to impact the receptor. The EIP of any county is calculated as:

$$\text{Equation (3): } EIP = \frac{E_p * D_0}{f(\text{distance})}$$

where

$E_p$  = county total emissions of pollutant  $p$

$D_0$  = spatial probability density at the county centroid

$f$  = function of distance between county and receptor

The EIP may be divided by a distance function to roughly account for dilution and increased uncertainty in model outputs far from the receptor site. However, for this study,  $f = 1$ . A geographic information system (GIS) tool was developed to calculate EIP values.

## RESULTS

### Nitrogen Oxides (NO<sub>x</sub>)

The NO<sub>x</sub> emission density by county (or equivalent for Canada, Mexico, and the Gulf of Mexico) is shown in Figure 3. Counties with high NO<sub>x</sub> emission density generally contain major cities or large point sources. Hercules Glades Wilderness is shown as a black square in southern Missouri.

**Figure 3.** NO<sub>x</sub> emission density by county or equivalent.

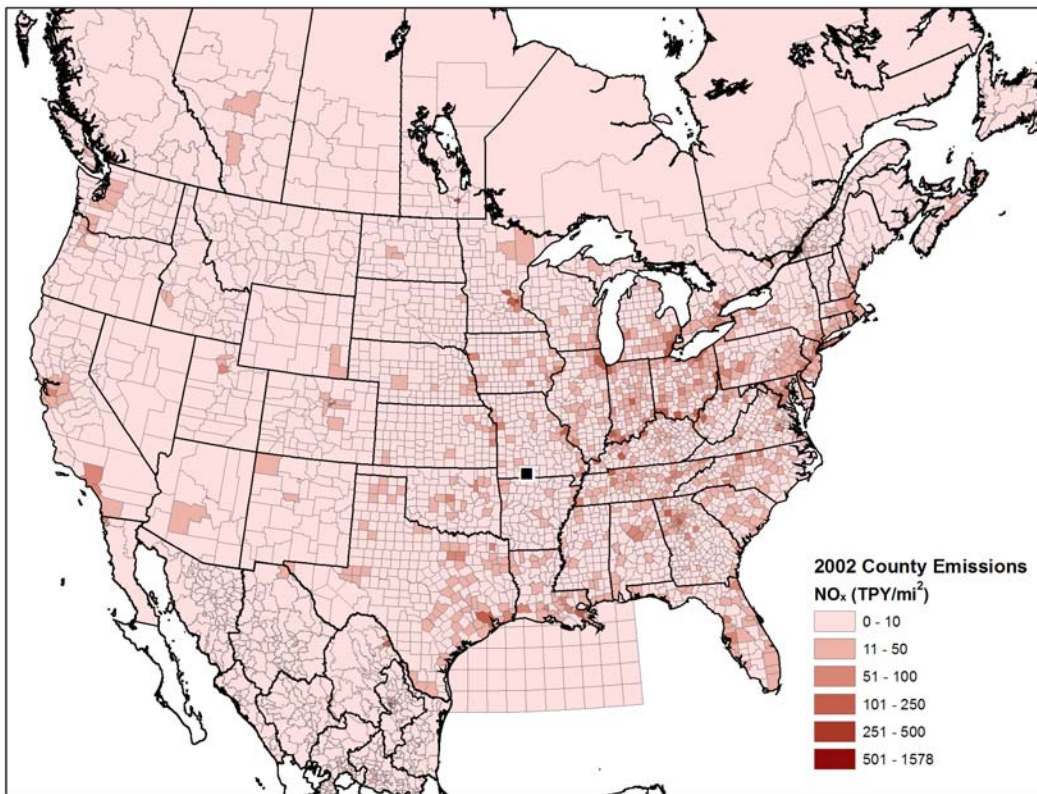
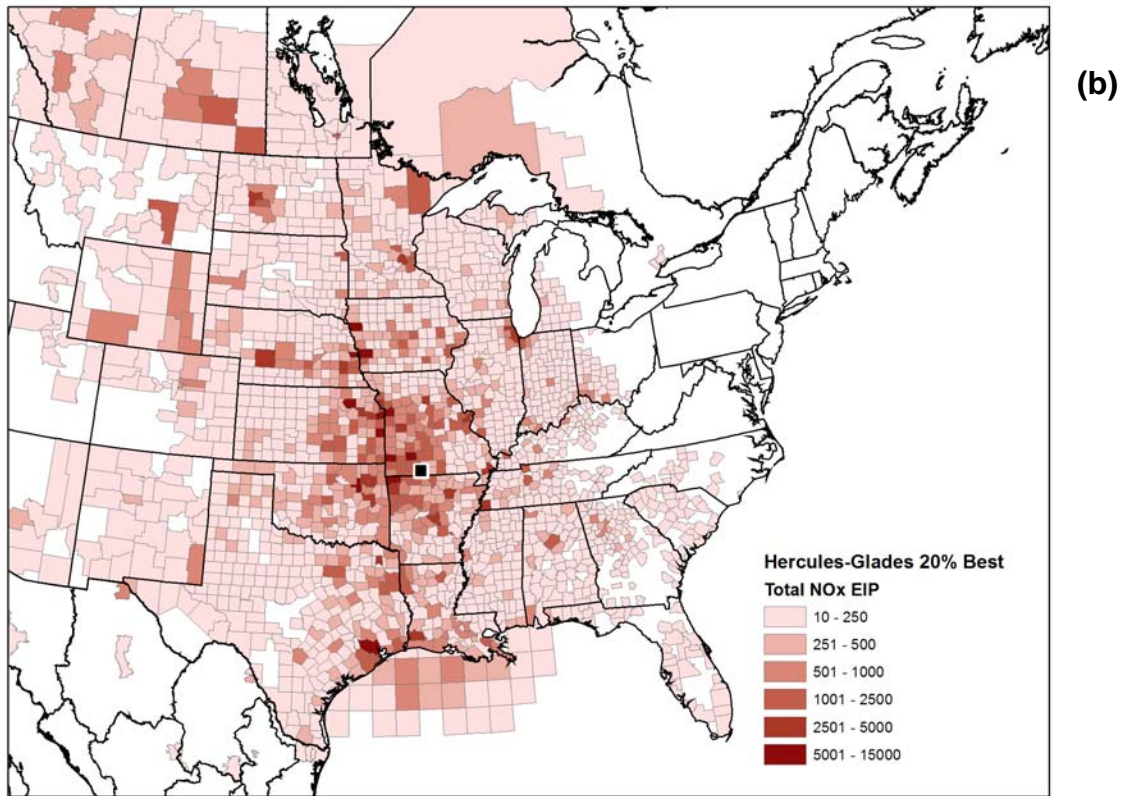
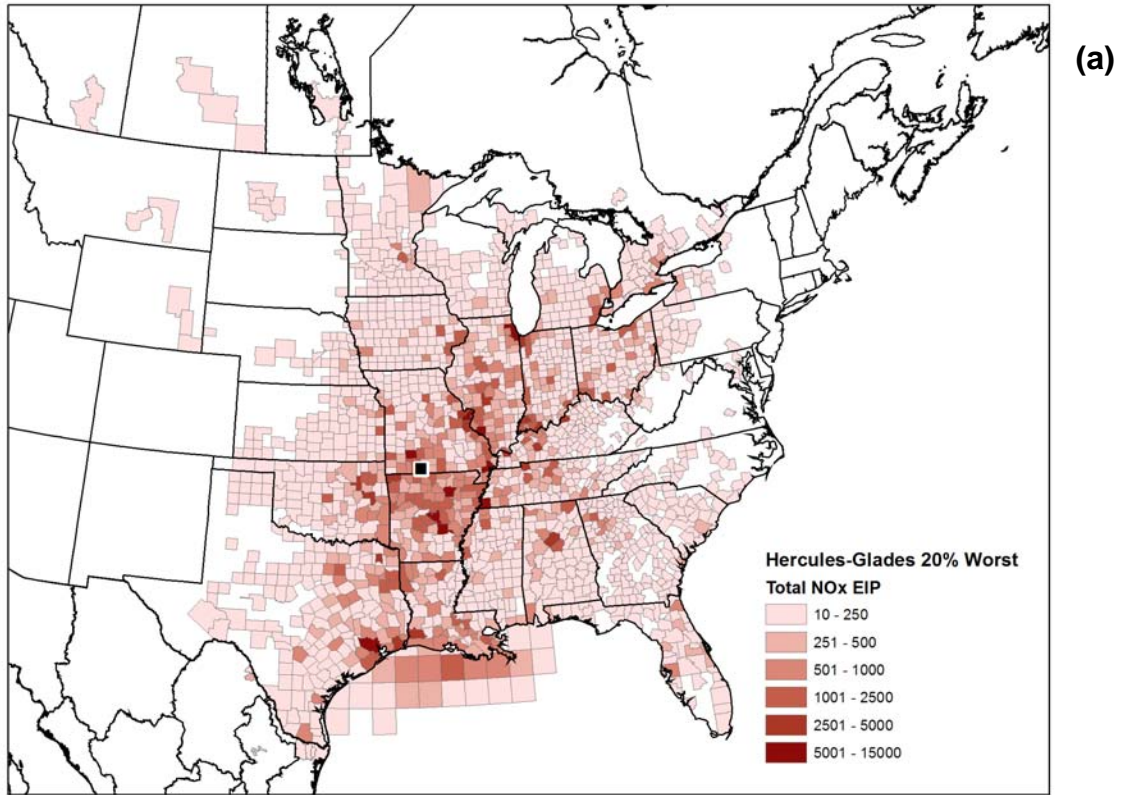
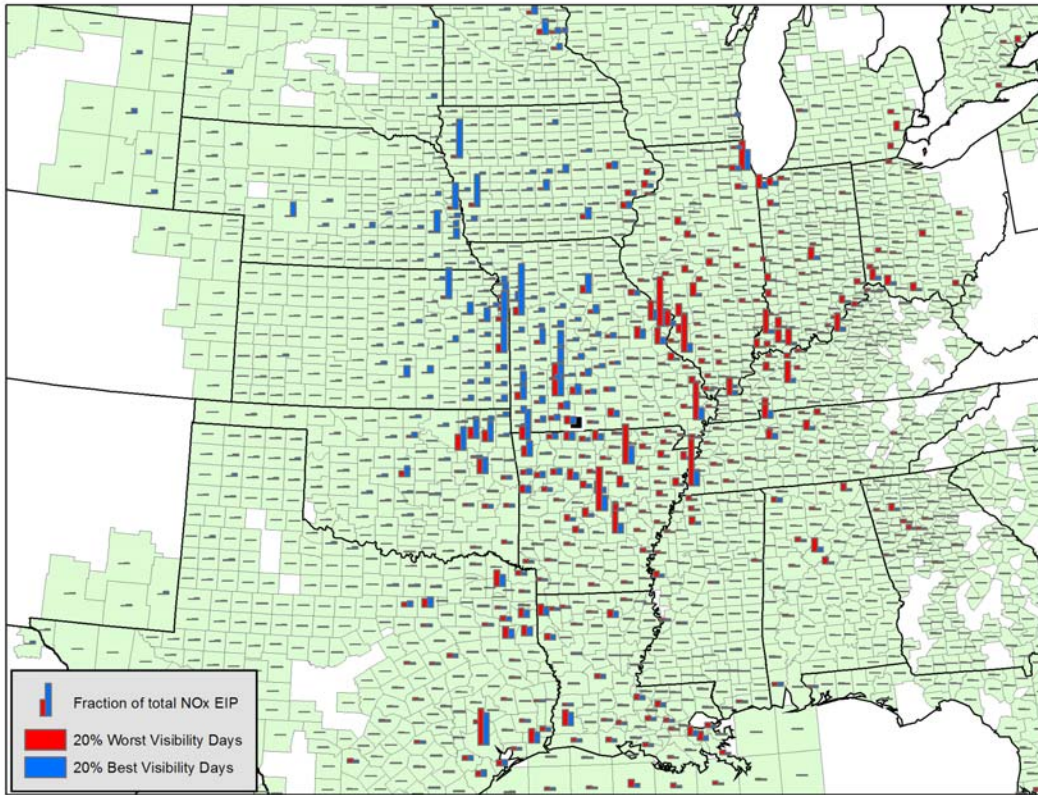


Figure 4 shows the NO<sub>x</sub> EIP values by county for the 20%-worst and 20%-best visibility days. When visibility at Hercules Glades is poor, trajectories are predominantly from the south and east, passing over areas of high NO<sub>x</sub> emission such as Texas, Louisiana, and the Ohio River Valley. On days with the best visibility, much of the airmass impacting Hercules Glades originates from the northwest, though winds from the south remain important. Figure 5 shows the fraction of total EIP for the best and worst visibility days on the same map, highlighting the spatial differences between the county-level NO<sub>x</sub> EIP. On the best visibility days, several counties along the Missouri river contribute the most to EIP. These counties are much less important on the worst visibility days. Overall, the EIP density (EIP divided by county area) is 7% higher on the worst visibility days than on the best days.

**Figure 4.** NO<sub>x</sub> EIP for the (a) 20%-worst days and (b) 20%-best days.



**Figure 5.** Fraction of total NO<sub>x</sub> EIP by county on the best and worst visibility days.



The emission inventory can also be queried by pollutant source types. Figure 6 shows the contribution to EIP aggregated to the state level, broken down by major source type (source classification code tier 1). The spatial pattern at the state level is similar to that at the county level. For the 20%-worst visibility days, 52% of total NO<sub>x</sub> EIP comes from the CENRAP domain, compared to 76% on the 20%-best visibility days. Though the NO<sub>x</sub> EIP on the best and worst visibility days varies spatially, the contributing source categories are nearly identical, with mobile sources making up about 50% of total EIP, and the remainder coming largely from point and area combustion sources. Table 2 lists the major contributing sources of NO<sub>x</sub> EIP at Hercules Glades.

**Figure 6.** State NO<sub>x</sub> EIP by source category on the (a) 20%-worst days and (b) 20%-best days.

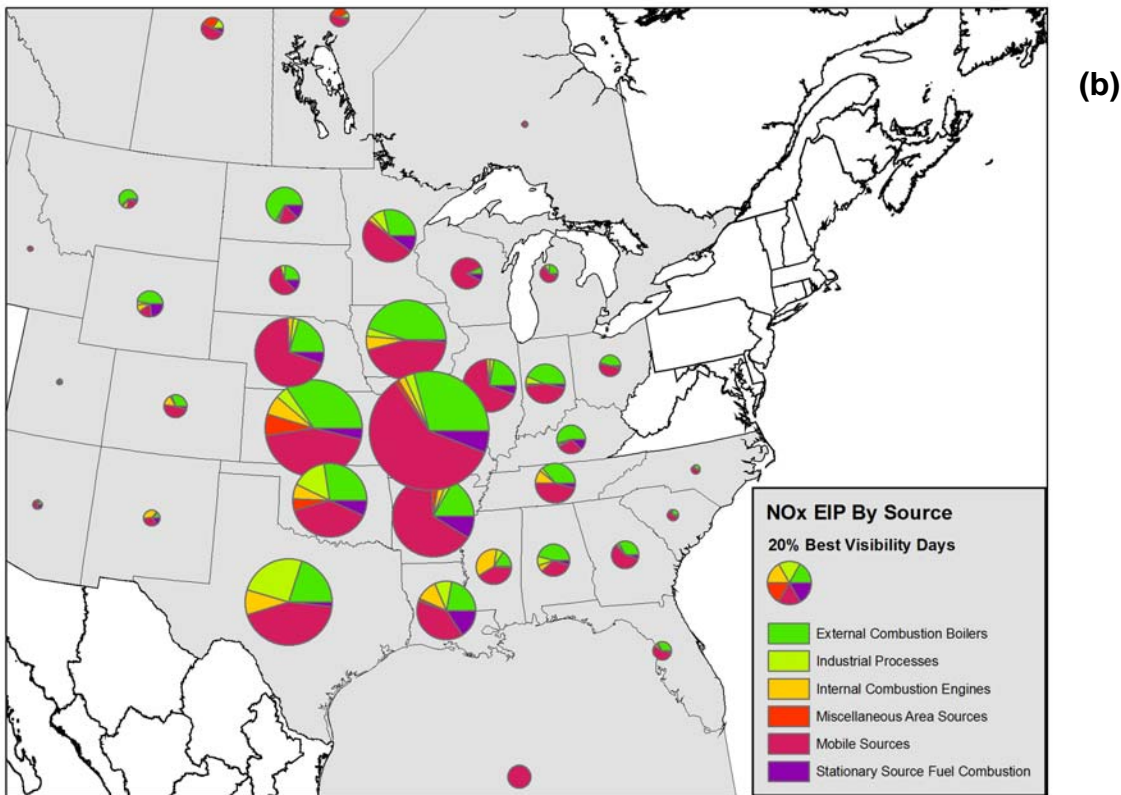
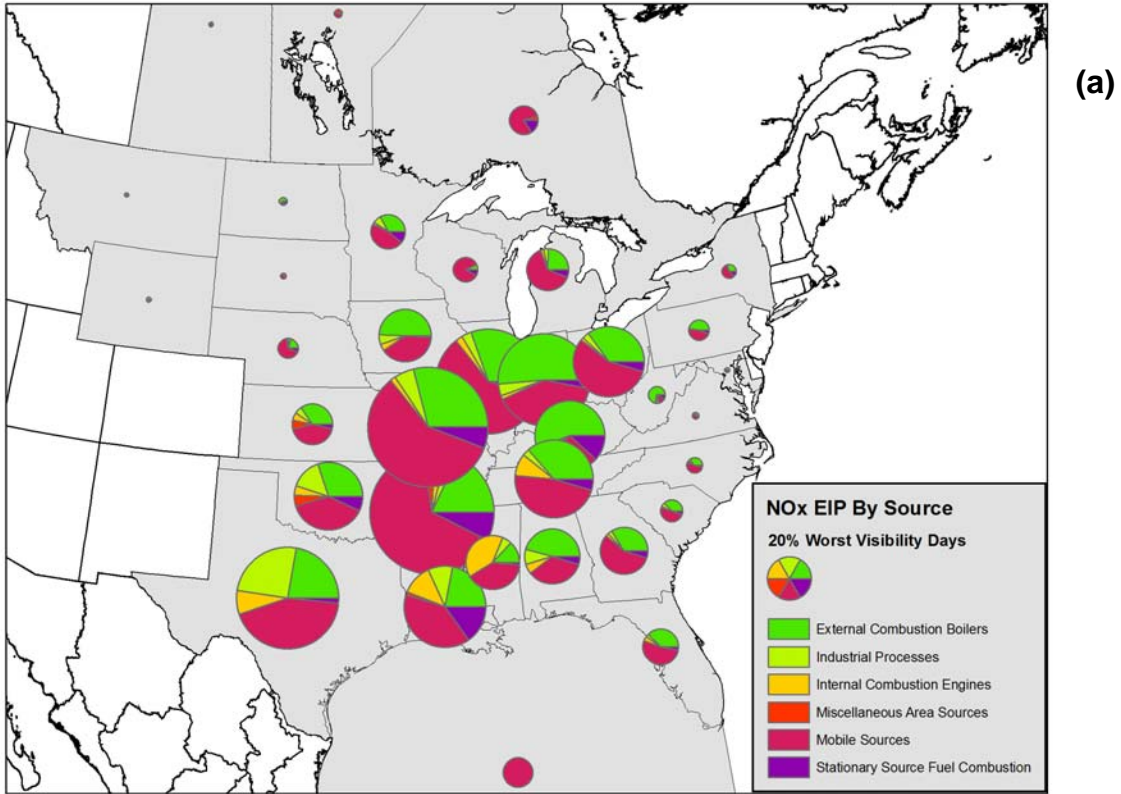


**Table 2.** Major sources of NO<sub>x</sub> EIP at Hercules Glades Wilderness.

Source	NO <sub>x</sub> EIP 20%-Worst Days (% of total)	NO <sub>x</sub> EIP 20%-Best Days (% of total)
Electric Generation	27	25
Gasoline Highway Vehicles	17	16
Diesel Highway Vehicles	17	15
Industrial Boilers/Engines	9	11
Off-highway Diesel Vehicles	6	8
Railroad Equipment	5	7
Commercial Marine Vessels	4	2
Oil and Gas Production	2	3
Mineral Products	2	2
Other	11	11

### **Sulfur Dioxide (SO<sub>2</sub>)**

The SO<sub>2</sub> emission density by county from the North American inventory is shown in Figure 7. The highest values are generally in counties with one or more significant point sources; these point sources dominate the SO<sub>2</sub> emission inventory.

Figure 8 shows the SO<sub>2</sub> EIP for the 20%-worst and 20%-best visibility days. Note that the trajectories used to calculate EIP for both NO<sub>x</sub> and SO<sub>2</sub> are identical so any differences in EIP between the two are due solely to differences in the emission inventory. For the 20%-worst days, high EIP values come from the south and east. For the 20%-best days, high EIP values mostly come from the north and west.

**Figure 7.** SO<sub>2</sub> emission density by county.

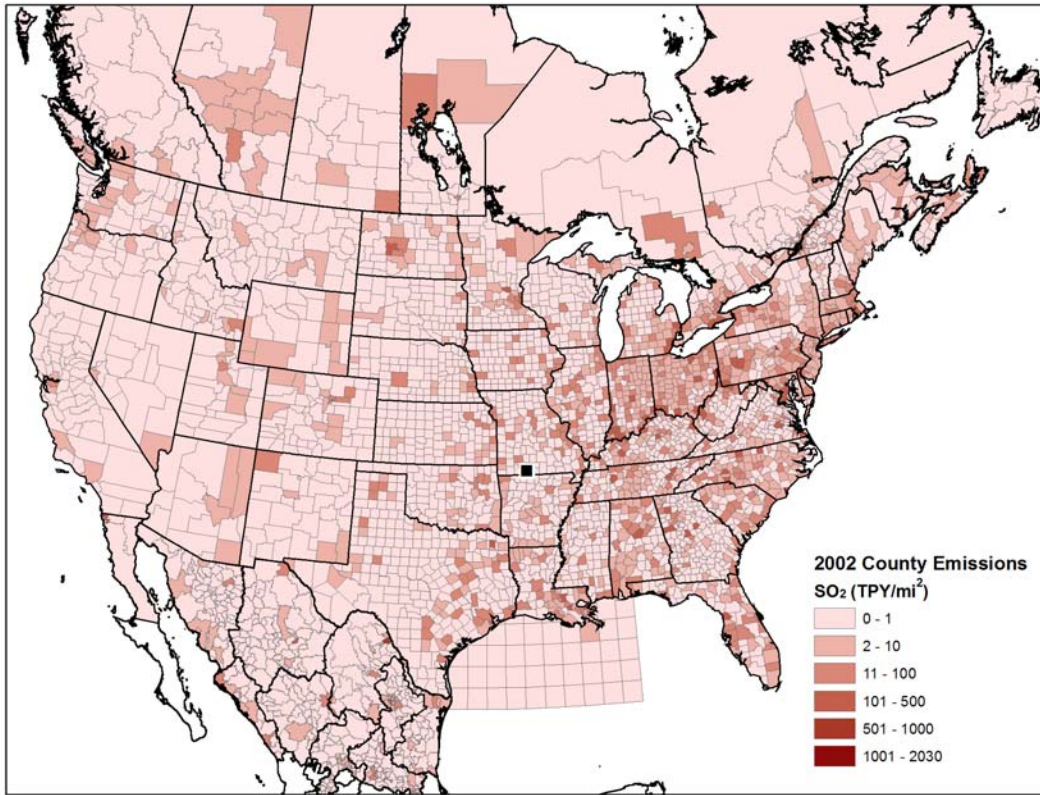


**Figure 8.** SO<sub>2</sub> EIP for the (a) 20%-worst days and (b) 20%-best days.

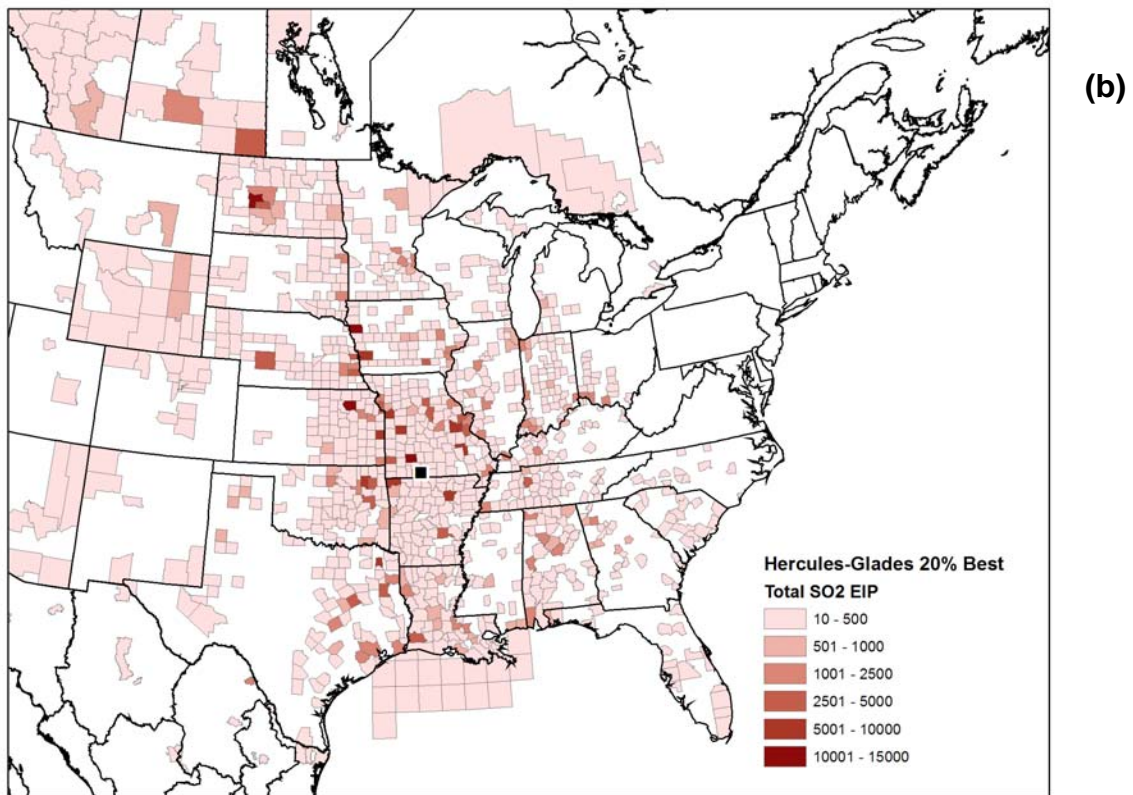
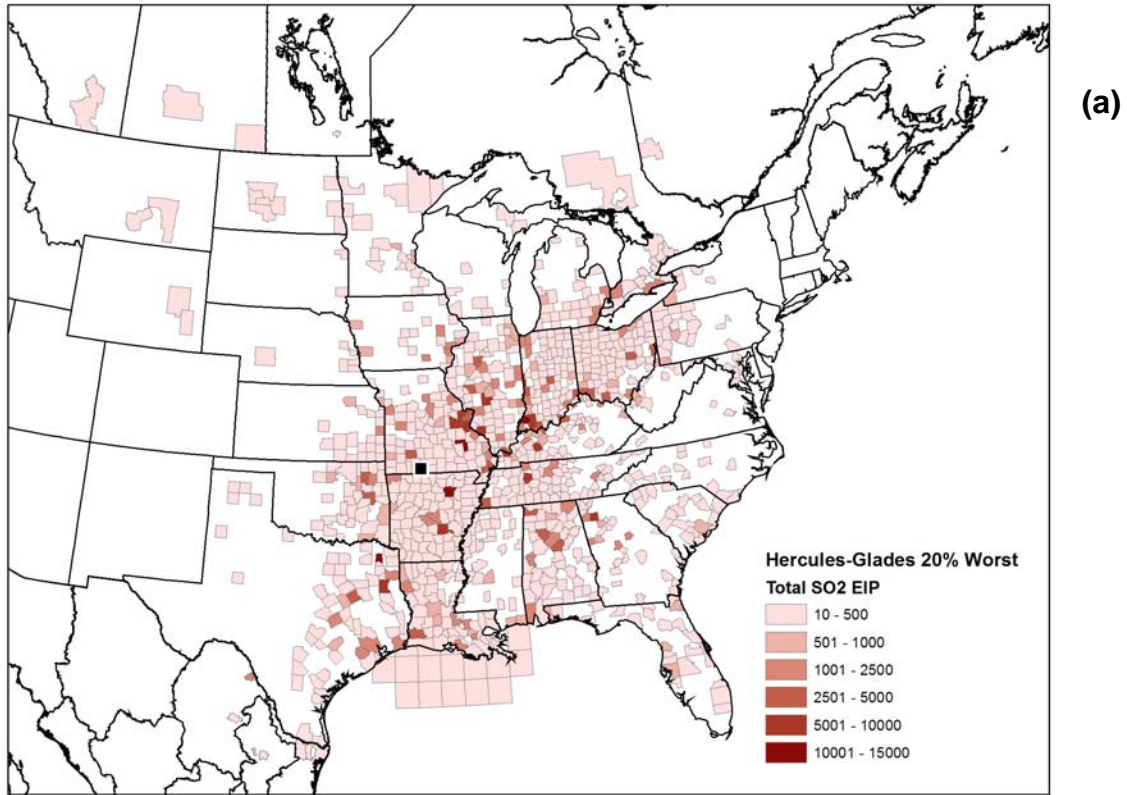
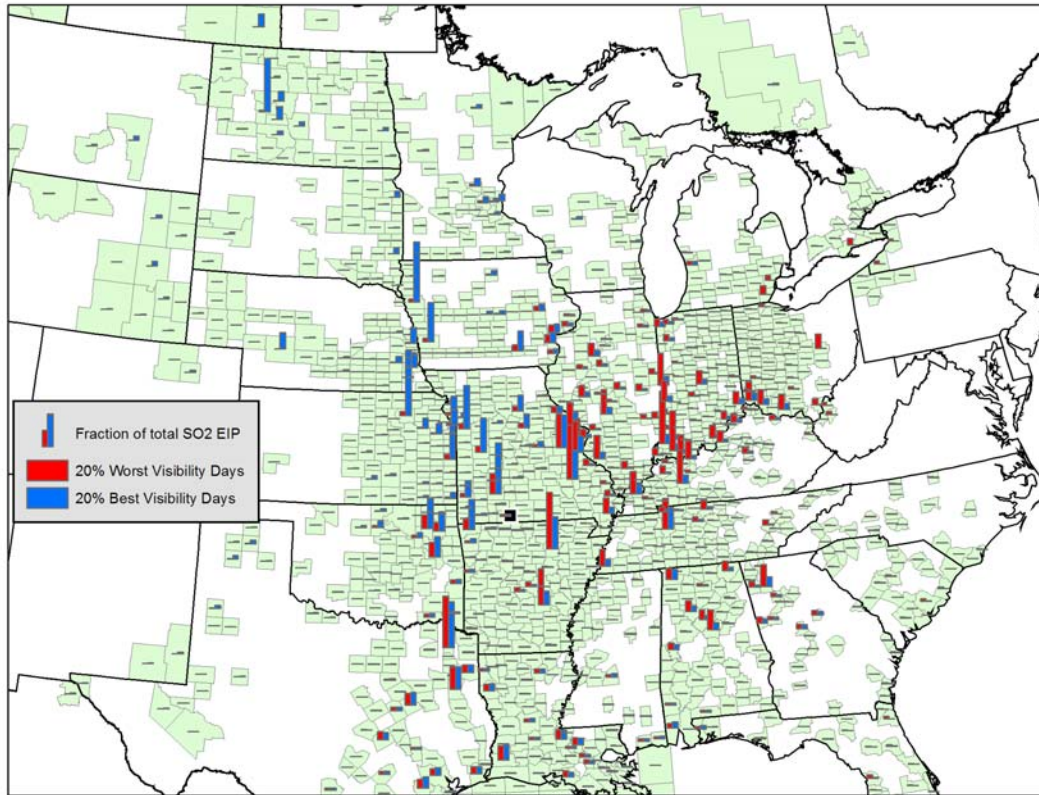


Figure 9 shows the spatial difference between SO<sub>2</sub> EIP on the best and worst visibility days. Counties with large SO<sub>2</sub> emissions are located on all sides of the site; however, the EIP density for the 20%-worst days is 40% higher than the EIP density on the 20%-best visibility days, i.e., the potential for SO<sub>2</sub> emissions to impact Hercules Glades according to this metric is consistent with observed visibility.

**Figure 9.** Fraction of total SO<sub>2</sub> EIP by county on the best and worst visibility days.



Aggregating the SO<sub>2</sub> EIP by state and showing contributions by source type reveals the dominance of point sources, particularly external combustion boilers (i.e., coal-fired power plants) as shown in Figure 10. This view also highlights the contributions from within and outside the CENRAP domain. The CENRAP states comprise 42% of the EIP on the worst visibility days and 69% on the best visibility days. The greatest contributing source types to the SO<sub>2</sub> EIP are shown in Table 3. Note that emissions associated with electric power generation account for greater than two-thirds of the total SO<sub>2</sub> EIP.

**Figure 10.** State SO<sub>2</sub> EIP by source category for the (a) 20%-worst days and (b) 20%-best days.

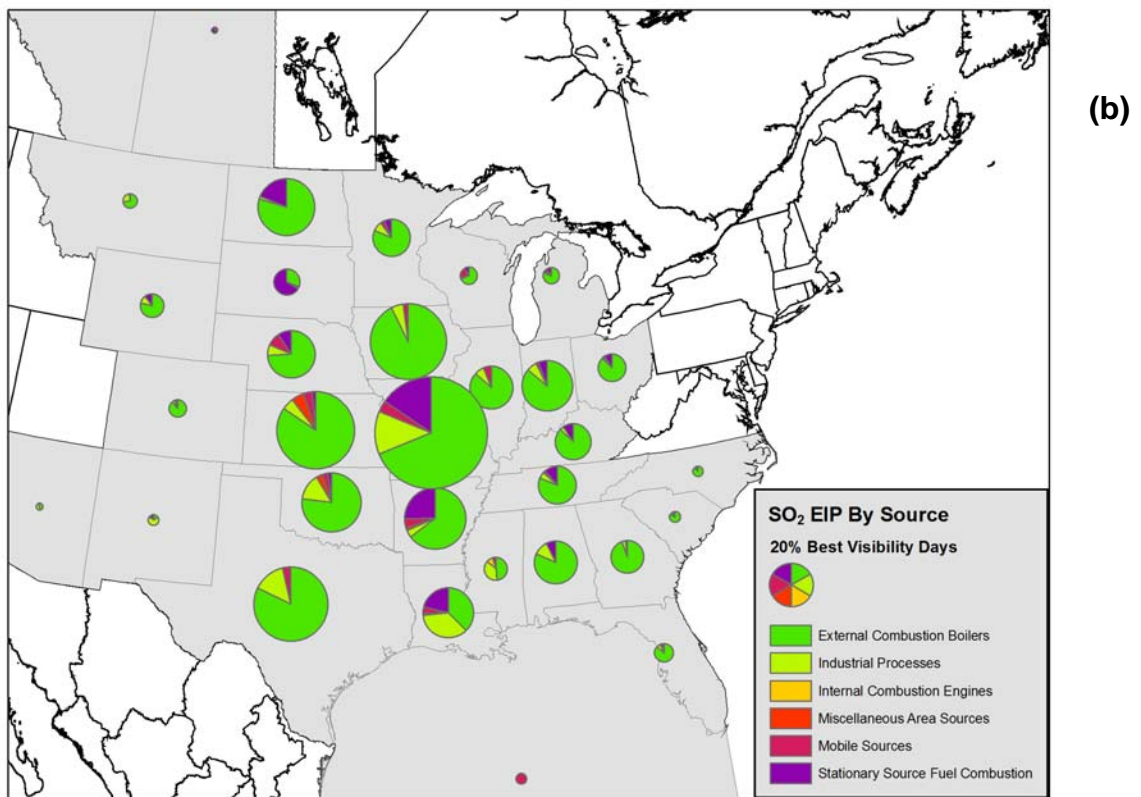
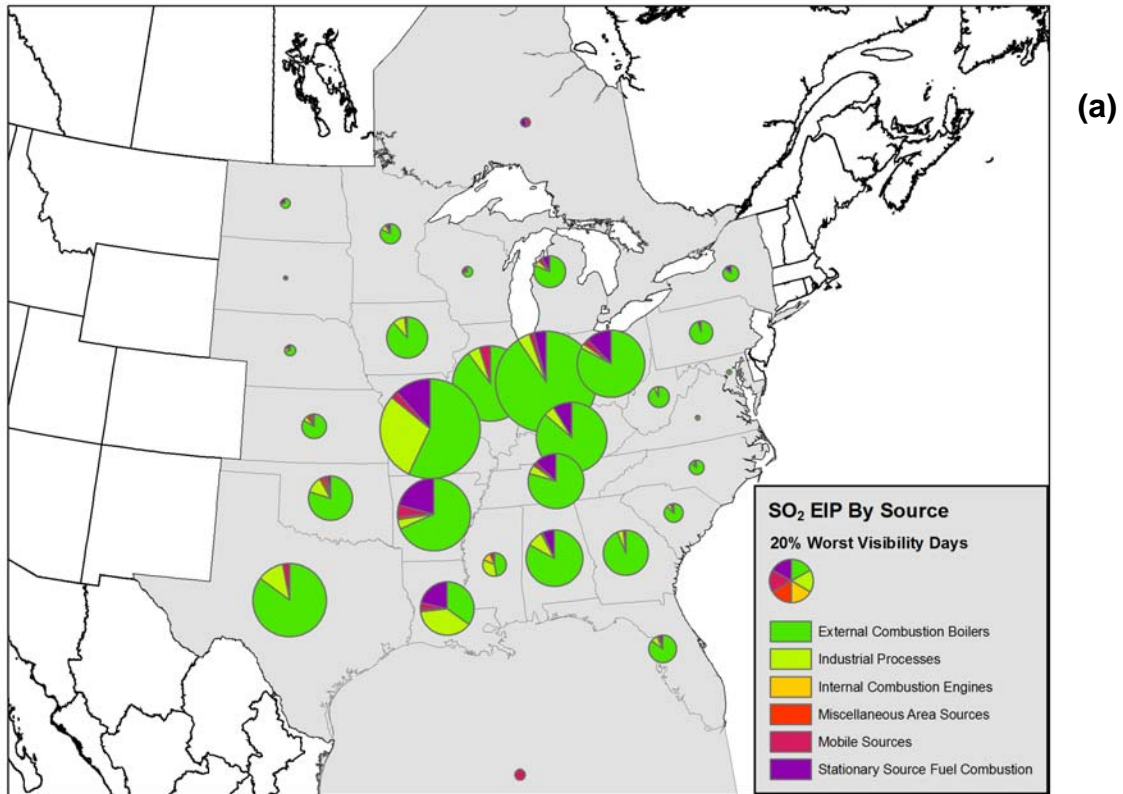


**Table 3.** Major sources of SO<sub>2</sub> EIP at Hercules Glades Wilderness.

Source	SO <sub>2</sub> EIP 20%-Worst Days (% of total)	SO <sub>2</sub> EIP 20%-Best Days (% of total)
Electric Power Generation	69	68
Industrial Combustion	9	15
Primary Metal Production	4	2
Mineral Products	2	2
Chemical Manufacturing	2	2
Petroleum Industry	2	2
Others	12	8

## DISCUSSION

SO<sub>2</sub> and NO<sub>x</sub> were chosen for this preliminary analysis because the emission inventory contained the most data for them. Hercules Glades Wilderness was chosen from several Class I sites within the CENRAP because visibility data were available for this site and a previous analysis<sup>9</sup> showed that the visibility at this site is driven primarily by sulfate. As the inventory is completed for other pollutants such as PM<sub>2.5</sub>, PM<sub>10</sub>, NH<sub>3</sub>, VOCs we would like to perform a similar EIP analysis for these pollutants and for several other sites that may have visibility issues driven by other components. Although relative source type contributions did not vary significantly between the best and worst visibility runs in this analysis, this may not be the case for other pollutants and/or sites. If they do vary, it would be useful to look at specific source categories that have the potential to install new controls.

Hercules Glades Wilderness had only a small difference between NO<sub>x</sub> EIP density for the 20%-worst and 20%-best visibility days, despite a substantial difference in the transport pattern. By contrast, the SO<sub>2</sub> EIP density was 40% higher for the 20%-worst visibility days. This analysis suggests that SO<sub>2</sub> EIP is a potential driver for poor visibility at the site. Since SO<sub>2</sub> is a precursor to sulfate, this is consistent with our understanding that sulfate is the primary cause of poor visibility at this site. It would be useful to calculate EIP density on a daily basis and explore its correlation with monitored visibility concentration.

On the 20%-best days, nearly 69% of SO<sub>2</sub> EIP is within the CENRAP domain. CENRAP has the opportunity to maintain the visibility on those days by not increasing emissions in upwind counties. This opportunity is not as strong for the 20%-worst days, with only 42% of EIP originating within the CENRAP states.

Once the tools have been developed, EIP analysis is simple and quick to perform and can be useful for characterizing how emissions affect receptors. However, this tool is not intended to replace photochemical modeling. It has been designed to neglect important complicating factors such as photochemistry and deposition. The numerical EIP value is a new metric, and quantitative assessments can only be made on a relative basis.

## CONCLUSIONS

EIP is a simple mathematical tool for combining meteorological data with emission inventory information to determine how emissions away from a site could be affecting pollutant concentrations at the site. EIP was calculated for SO<sub>2</sub> and NO<sub>x</sub> for Hercules Glades Wilderness in southern Missouri. According to the analysis, SO<sub>2</sub> EIP is a better predictor of visibility at this site than NO<sub>x</sub>. Further analyses will explore other pollutants and sites.

## REFERENCES

1. Gebhart, K. A.; Kreidenweis, S. M.; Malm, W. C. "Back-trajectory analyses of fine particulate matter measured at Big Bend National Park in the historical database and the 1996 scoping study", *Sci. Total Environ.* 2001, 276(Issues 1-3), 185-204.
2. Gebhart, K. A.; Malm, W. C.; Flores, M. "A preliminary look at source-receptor relationships in the Texas-Mexico border area", *J. Air & Waste Manage. Assoc.* 2000, 50, 858-868.
3. Ashbaugh, L. L.; Malm, W. C.; Sader, W. Z. "A residence time probability analysis of sulfur concentrations at Grand Canyon National Park", *Atmos. Environ.* 1985, 19(8), 1263-1270.
4. Sturman, A.; Zawar-Reza, P. "Application of back-trajectory techniques to the delimitation of urban clean air zones", *Atmos. Environ.* 2002, 36(20), 3339-3350.
5. Brown, S. G.; Frankel, A.; Raffuse, S. M.; Hafner, H. R.; Anderson, D. J. "Source apportionment of PM<sub>2.5</sub> in Phoenix, Arizona, using Positive Matrix Factorization", *J. Air & Waste Manage. Assoc.* 2004.
6. Draxler, R. R.; Hess, G. D. "Description of the Hysplit 4 modeling system"; ERL ARL-224, Technical memorandum by NOAA. 1997.
7. McCoy, J.; Johnston, K. "Using ArcGIS Spatial Analyst"; ESRI. 2001.
8. Cressie, N. A. C. *Statistics for Spatial Data*; John Wiley & Sons, Inc., 1993.
9. Brown, S. G.; Frankel, A.; Hafner, H. R.; Roberts, P. T.; Anderson, D. A. "Source Apportionment of PM<sub>2.5</sub> in Phoenix, Arizona with Positive Matrix Factorization", Presented at 2005 Particulate Matter Supersites Program and Related Studies: An AAAR International Specialty Conference, February 7-11, Atlanta, GA, 2005; STI-2687.

**KEY WORDS**

HYSPLIT

Emission inventory

Trajectory density

CENRAP

Regional Haze

Visibility